Multi-strain disease dynamics on a metapopulation network

Matthew Michalska-Smith[1] and Meggan E Craft[2]

[1]University of Minnesota
[2]Affiliation not available

June 11, 2019

Abstract

Many of the most impactful diseases that affect humans, livestock, and wildlife have clusters in their population-genetic variability that we classify as strains. Importantly, host immunity to one of these strains is neither independent from nor equivalent to immunity to related strains. This partial cross-protective immunity affects disease dynamics across the population as a whole and can dramatically influence intervention strategies. While the study of multi-strain diseases goes back decades, this work has not yet been generalized to a loosely connected collection of subpopulations, i.e. a metapopulation. Starting from the strain theory of host-pathogen systems proposed by Gupta (1998), we simulate multi-strain disease dynamics on a network of interconnected populations, characterizing the effects of parameterization and network structures on these dynamics. We find that dynamics propagate through the metapopulation network, even if parameters vary between populations. Moreover, in chains of connected populations experiencing cyclical dynamics, the movement of (partially) immune individuals dampens the dynamics of populations further along the chain. This work serves as an important first step in extending prior results on multi-strain diseases to a generalized population structure. This extension is particularly apt in the case of livestock production, where a system of mostly isolated populations (farms) is connected through the forced movement of individuals.

1 Introduction

Many of the most impactful infectious diseases that affect humans, livestock, and wildlife have clusters in their population-genetic variability that we classify as strains. Such variation in pathogen genotype often leads to differences in phenotype as well, importantly affecting the efficacy of host immune defenses. While the human immune system is usually capable of preventing re-infection with a pathogen to which it has been previously exposed, sufficient evolution on the part of the pathogen can lead to reduced recognition by the host. In some cases, this change is not sufficient to completely avoid recognition, however, leading to an immune response that is neither as strong as would be in the case of re-exposure to the same strain, nor as weak as in the case of exposure to a novel pathogen. This partial cross-protective immunity can lead to reduced transmission as well, affecting disease dynamics across the population.

Malaria, Cholera, Human Papillomavirus Virus, Dengue, Porcine Reproductive and Respiratory Syndrome, Brucellosis, *etc.* have strain structure, but differ in both the number of strains and the level of cross-protective immunity afforded by past exposure to similar strains. Perhaps the most well-studied example is that of Influenza (flu), a viral respiratory tract infection that counts humans among its many potential hosts and has substantial economic and public health consequences worldwide (Molinari et al., 2007; Fan et al., 2016; Peasah et al., 2013).

While the study of multi-strain diseases goes back decades, this work has not yet been generalized to a loosely connected collection of sub-populations, *i.e.* a metapopulation. Initially introduced through the concepts of island biogeography, this idea can be generalized to a variety of systems, including human movement between cities, livestock transport between farms, and populations living in fragmented natural habitats. In each case, there exist relatively high-density areas which are connected to one another through a network of individuals' movement. This framework allows the application of network analyses that can characterize patterns of connection within the population as a whole.

Historically, metapopulation studies have been been divided into two main camps: those that model within-patch dynamics and "cell occupancy" models in which only the presence or absence

of a given species within a patch is recorded (Taylor, 1988), with the latter receiving much more theoretical attention. Importantly, this latter case rests on an assumption of temporal separation in which local dynamics occur on a timescale that can be treated as instantaneous relative to that of the between-patch dynamics (Hanski, 1994). When considering diseases in systems with relatively high migration rates, however, this assumption rarely holds and the presence-absence approach can significantly affect model accuracy, especially when individual disease status might affect migration rates.

Here, we build on the strain theory of host-pathogen systems proposed by Gupta (1998), considering the case where a collection of populations undergoing local dynamics are furthermore interconnected through the movement of individuals between populations. We simulate disease dynamics on this system, characterizing the effects of parameterization and network structures on these dynamics. This work is divided into three sections: first, we explore the simple case of interconnected populations with identical parameterizations. Second, we consider the case in which parameters differ between populations. Finally, we explore the case of a larger network of connected populations, looking at the role of network structure on key measures of disease progression.

2 Methods

2.1 Model framework for one population

We work from a system of ordinary differential equations detailing the proportion of a population in classes based on current and past exposure to different strains of a pathogen. We signify a strain $i = \{x_1, x_2, \ldots, x_n\}$ as a set of n loci, each of which can take on a finite number of alleles. For instance, a pathogen with two loci (a and b) and two alleles at each loci has a total of four potential strains: $\{a_1, b_1\}$, $\{a_1, b_2\}$, $\{a_1, b_1\}$, $\{a_2, b_2\}$. Importantly, in this model framework, the number of strains is fixed and finite. While strains may go extinct over time, there is no process for the generation of new strains or to re-introduce strains that had previously gone extinct (Gupta, 1998, but see).

The model consists of sets of three nested equations (one set for each strain): w, z, and y, where

each set consists of as many equations as there are strains. w_i represents the proportion of the population which has been exposed to a strain j of the pathogen, where strain j has at least one allele in common with strain i, *i.e.*, $j \cap i \neq \emptyset$. z_i represents the proportion of the population that has been exposed to strain i itself. Finally, y_i represents that proportion of the population currently infected with strain i (and thus capable of infecting others). Thus, the proportion of the population in y_i is also in z_i and the proportion of the population in z_i is also in w_i, and $y_i \leq z_i \leq w_i$. The y class is analogous to the I class in standard SI, SIR, *etc.* single-strain frameworks, while w and z are composed of combinations of I and R classes. The susceptible population is not modeled explicitly in this framework.

These equations have the form:

$$\begin{aligned}
\frac{\mathrm{d}y_i}{\mathrm{d}t} &= \beta\left((1-w_i)+(1-\gamma)(w_i-z_i)\right)y_i - \sigma y_i - \mu y_i \\
\frac{\mathrm{d}z_i}{\mathrm{d}t} &= \beta(1-z_i)y_i - \mu z_i \\
\frac{\mathrm{d}w_i}{\mathrm{d}t} &= \beta(1-w_i)\sum_{j \ni j \cap i \neq \emptyset} y_j - \mu w_i
\end{aligned} \tag{1}$$

Where, as above, we denote strains as subscripts and in the equation for w_i we sum over all strains j which share at least one allele with the focal strain i. β, σ, and μ are the infection, recovery, and death rates, respectively. γ is an indicator of the level of cross-protective immunity gained by prior exposure to alleles in the target strain. Note that while we depict only one value per demographic parameter (*i.e.*, all strains are functionally equivalent) for notational clarity, these values could also vary by strain (*e.g.*, β_i) in this framework.

Note that immunity in this framework is non-waning: exposure to a strain yields consistent protection from future infection over the lifespan of the individual. The level of this infection is dichotomous: with respect to the same strain, it is complete protection, with respect to any strain sharing at least one allele, it modifies infection risk according to the parameter γ. Importantly, we also do not distinguish between loci, assuming that sharing an allele at any locus is functionally identical to sharing an allele at any other locus.

2.2 Extensions to consider more than one population

Following Xiao et al. (2011), we model movement between populations using a dispersal matrix $\Delta = \mathrm{A} - \mathrm{E}$, where A is the weighted adjacency matrix indicating the proportion of individuals moving from from patch i (row) to patch j (column) and E is a diagonal matrix representing emigration, where each entry $\mathrm{E}_{jj} = \sum_{i=1}^{n} \mathrm{A}_{ij}$ where n is the number of patches. Thus, the whole system can be depicted by a set of three equations for each strain i in each patch k:

$$\begin{aligned}
\frac{\mathrm{d}y_{i,k}}{\mathrm{d}t} &= \beta\left((1-w_{i,k}) + (1-\gamma)(w_{i,k}-z_{i,k})\right) y_{i,k} - \sigma y_{i,k} - \mu y_{i,k} + \sum_{l} \Delta_{kl} y_{j,l} \\
\frac{\mathrm{d}z_{i,k}}{\mathrm{d}t} &= \beta(1-z_{i,k}) y_{i,k} - \mu z_{i,k} + \sum_{l} \Delta_{kl} z_{j,l} \\
\frac{\mathrm{d}w_{i,k}}{\mathrm{d}t} &= \beta(1-w_{i,k}) \sum_{j \ni j \cap i \neq \emptyset} y_{j,k} - \mu w_{i,k} + \sum_{l} \Delta_{kl} w_{j,l}
\end{aligned} \tag{2}$$

Where each equation is now additionally indexed according to population. While in principle the elements of Δ can take any value $[0, 1]$, signifying a movement of between 0 and 100% of individuals, for simplicity we use a constant value of $\delta = 0.1$ for the strength of each movement. Sensitivity to this value is explored in the Supplementary Information.

Note that this formulation assumes uniform sampling for migration between populations. One might imagine cases in which currently infectious individuals are less likely to migrate than those who have recovered and now have immunity. We explore this variation in migration structure in the Supplementary Information.

This framework can be applied to a metapopulation of arbitrary size and complexity. Fundamentally, the dynamics of each population will be governed by a set of three equations per disease strain, and these equations are interlinked within a population by partial, cross-protective immunity, and between populations through a network specifying movement of individuals between patches. Thus, the total number of differential equations for any given system will be 3 x the number of strains x the number of patches in the metapopulation.

2.3 Simulation Prodedure

All simulations were carried out in Julia (Bezanson et al., 2017), with graphics produced using the ggplot package (Wickham, 2016) in R (R Core Team, 2019). In addressing the first two objectives mentioned above, we fix the values of all variables other than γ (the degree of cross-protective immunity) and Δ (the network of movement information). The former is varied to demonstrate the variety of dynamics obtainable in this modeling framework (as in Gupta (1998)), while the latter varies the number and interconnections of the network patches.

For each of the following simulations, we assume that there is no mortality, but add movement out of each sink population to balance in- and out-flows in the system. This simplification does not qualitatively change the dynamics of the system.

For Figure 1, we use a movement network described by a chain of populations, *i.e.* $A \to B \to C \to D$ or

$$\Delta = \begin{bmatrix} -\delta & \delta & 0 & 0 \\ 0 & -\delta & \delta & 0 \\ 0 & 0 & -\delta & \delta \\ 0 & 0 & 0 & -\delta \end{bmatrix},$$

where $\delta = 0.1$.

For figure 2, we restrict our consideration to a system of two patches, identical in all respects other than the parameter γ, which is set to either induce a steady state of coexistence ($\gamma = 0.25$ in population A) or cyclical coexistence ($\gamma = 0.75$ in population B). We then display three potential patterns of connection: $A \to B$ (right column), $B \to A$ (left column), and the case of no migration between patches (middle column). Specifically, we set

$$\Delta = \begin{bmatrix} -\delta & \delta \\ 0 & -\delta \end{bmatrix}, \Delta = \begin{bmatrix} -\delta & 0 \\ \delta & -\delta \end{bmatrix}, \text{and } \Delta = \begin{bmatrix} -\delta & 0 \\ 0 & -\delta \end{bmatrix},$$

respectively.

Finally, for figure 3, we consider a system of three populations: $A \rightarrow C \leftarrow B$, or

$$\Delta = \begin{bmatrix} -\delta & 0 & \delta \\ 0 & -\delta & \delta \\ 0 & 0 & -\delta \end{bmatrix},$$

where populations A and C have $\gamma = 0.25$, but population B has $\gamma = 0.75$.

3 Results

3.1 Dynamics are dampened along chains in the metapopulation network

We find that even when all populations share the same parameterizations and initial conditions, that populations further along network chains have dampened oscillatory dynamics compared to those they would exhibit in isolation (FIgure 1). This is likely due to the movement of (partially) immune individuals between the populations, increasing the proportion of specific and cross-reactively immune individuals in populations further along the chain. While infectious individuals move at an equal rate, the proportion of the population that is currently infectious at any given time is much smaller than the proportion with immunity.

3.2 Dynamics propagate through metapopulation networks

We find that in the case of a simple chain of populations, the dynamics of sink populations can be overridden by the dynamics of source populations (Figure 2). Interestingly, this is true both of cyclical dynamics overruling stable dynamics and *vice versa*. In the case of multiple source populations, cycles tend to dominate over stable dynamics. Importantly, this migration can allow for strain coexistence even in populations where the disease parameters would suggest extinction of one or more strains.

3.3 There exists a dynamics hierarchy

The issue of dynamics propagation gets more complicated when there are multiple, varying source populations for a given sink population. We find that there is a hierarchy of dynamics in their propagation through the network: cyclical dynamics overpower steady states and chaos overpowers

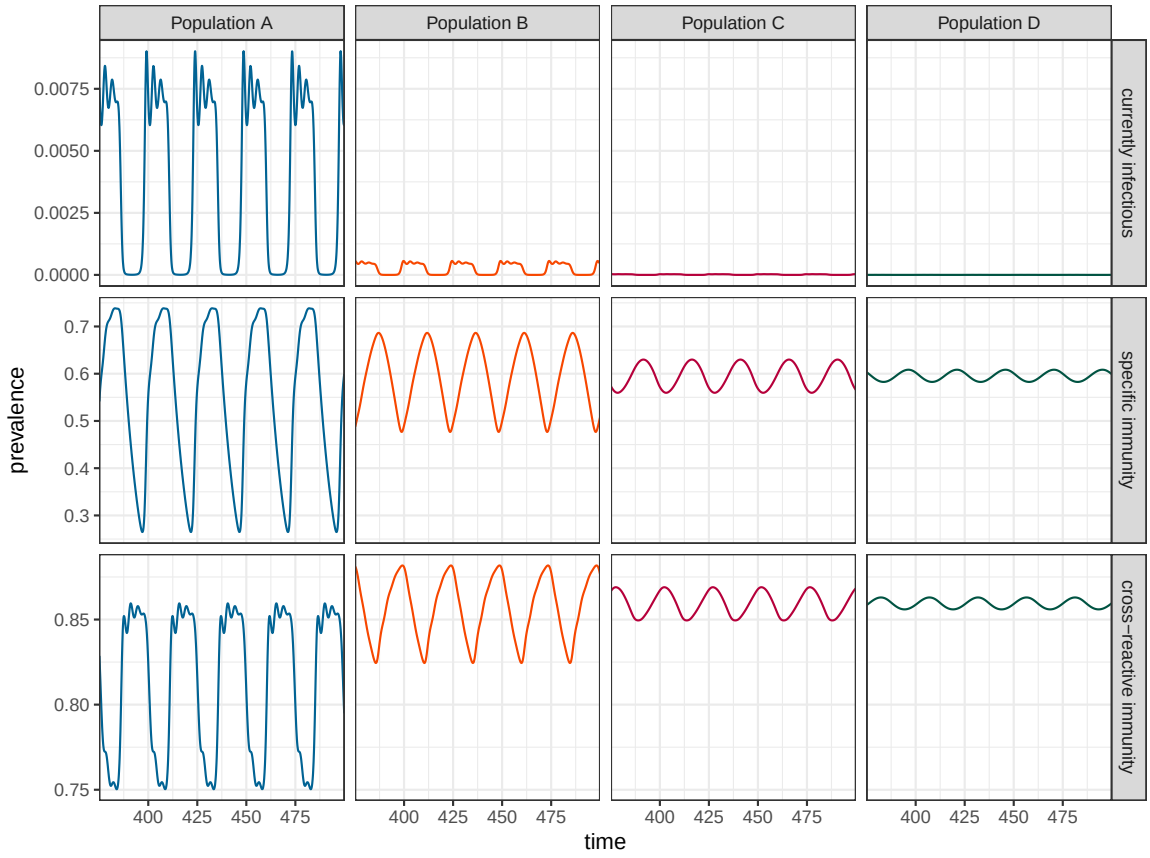

Figure 1: Connecting multiple populations with the same dynamics results in dampened clycles in populations further down the chain. Here, populations are connected such that $A \rightarrow B \rightarrow C \rightarrow D$. Importantly, the mean level of immunity (cross-reactive and specific) increases in each sequential population, while the mean level of currently infectious decreases. All populations have parameters $\beta = 40,\ \sigma = 10,\ \mu = 0,\ \delta = 0.1,\ \gamma = 0.75$. The strain structure consists of two loci with two alleles at each. Here, we show only one strain's dynamics for clarity.

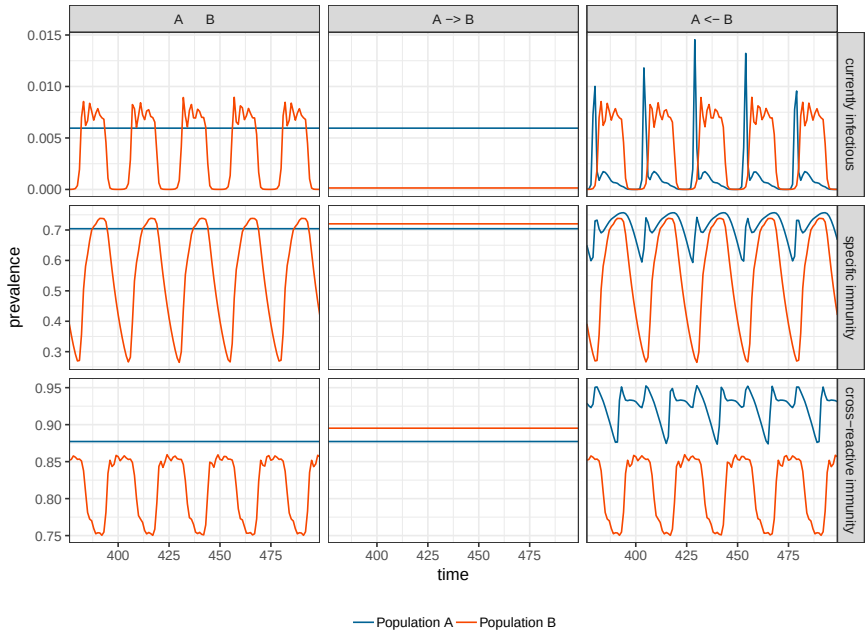

Figure 2: The effect of linking populations with different model parameterizations. While in isolation (center column), population A has steady-state dynamics and population B has cyclical dynamics, when the two populations are linked by migration, the sink population inherits the dynamics of the source population (left and right columns). This is true regardless of the direction of the movement. Populations have parameters $\beta = 40,\ \sigma = 10,\ \mu = 0,\ \delta = 0.1$ in common and $\gamma = 0.25,\ 0.75$ respectively. As before, we use a two-loci, two-allele strain structure, but show only one strain for clarity.

cycles, regardless of any imbalance in the relative contributions of the sources. Put another way, if just one of many source populations (or a small proportion of the total movement) has cyclical dynamics, the sink population will also have cyclical dynamics.

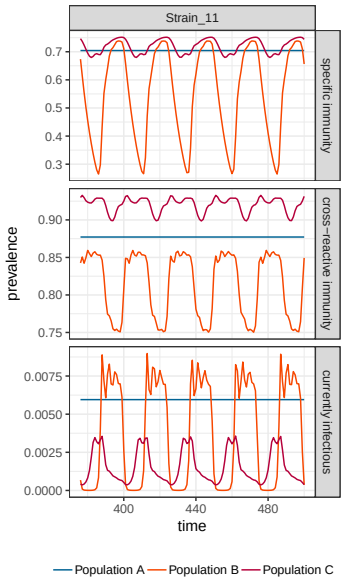

Figure 3: The effect of multiple source populations with differing dynamics on the sink population. Here, we have populations A and B feeding into population C at the same rate of $\delta = 0.1$. Populations A and C show steady state dynamics, with $\beta = 40$, $\sigma = 10$, $\mu = 0$, $\gamma = 0.25$. Population B shows cyclical dynamics with $\gamma = 0.75$ and all other parameters the same. Note that, even though the parameters of population C would lead to steady state in the absence of migration, we see cyclical dynamics being inherited from population B.

References

Jeff Bezanson, Alan Edelman, Stefan Karpinski, and Viral B. Shah. Julia: A Fresh Approach to Numerical Computing. *SIAM Review*, 59(1):65–98, jan 2017. doi: 10.1137/141000671. URL https://doi.org/10.1137%2F141000671.

Victoria Fan, Dean Jamison, and Lawrence Summers. The Inclusive Cost of Pandemic Influenza Risk. Technical report, mar 2016. URL https://doi.org/10.3386%2Fw22137.

S. Gupta. Chaos Persistence, and Evolution of Strain Structure in Antigenically Diverse Infectious

Agents. *Science*, 280(5365):912–915, may 1998. doi: 10.1126/science.280.5365.912. URL https://doi.org/10.1126%2Fscience.280.5365.912.

Ilkka Hanski. A Practical Model of Metapopulation Dynamics. *The Journal of Animal Ecology*, 63 (1):151, jan 1994. doi: 10.2307/5591. URL https://doi.org/10.2307%2F5591.

Noelle-Angelique M. Molinari, Ismael R. Ortega-Sanchez, Mark L. Messonnier, William W. Thompson, Pascale M. Wortley, Eric Weintraub, and Carolyn B. Bridges. The annual impact of seasonal influenza in the US: Measuring disease burden and costs. *Vaccine*, 25(27):5086–5096, jun 2007. doi: 10.1016/j.vaccine.2007.03.046. URL https://doi.org/10.1016%2Fj.vaccine.2007.03.046.

Samuel K. Peasah, Eduardo Azziz-Baumgartner, Joseph Breese, Martin I. Meltzer, and Marc-Alain Widdowson. Influenza cost and cost-effectiveness studies globally – A review. *Vaccine*, 31(46): 5339–5348, nov 2013. doi: 10.1016/j.vaccine.2013.09.013. URL https://doi.org/10.1016%2Fj.vaccine.2013.09.013.

R Core Team. *R: A Language and Environment for Statistical Computing*. R Foundation for Statistical Computing, Vienna, Austria, 2019. URL https://www.R-project.org/.

Andrew D. Taylor. Large-scale spatial structure and population dynamics in arthropod predator-prey systems. *Annales Zoologici Fennici*, pages 63–74, 1988.

Hadley Wickham. *ggplot2: Elegant Graphics for Data Analysis*. Springer-Verlag New York, 2016. ISBN 978-3-319-24277-4. URL https://ggplot2.tidyverse.org.

Y. Xiao, Y. Zhou, and S. Tang. Modelling disease spread in dispersal networks at two levels. *Mathematical Medicine and Biology*, 28(3):227–244, September 2011. doi: 10.1093/imammb/dqq007. URL https://doi.org/10.1093%2Fimammb%2Fdqq007.